IOPscience iopscience.iop.org

Home Search Collections Journals About Contact us My IOPscience

Looking for the maximum low-temperature conductivity in selectively doped $Al_xGa_{1-x}As - GaAs - Al_xGa_{1-x}As$ double heterojunctions

This article has been downloaded from IOPscience. Please scroll down to see the full text article.

1996 J. Phys.: Condens. Matter 8 L421

(http://iopscience.iop.org/0953-8984/8/30/002)

View the table of contents for this issue, or go to the journal homepage for more

Download details:
IP Address: 171.66.16.206
The article was downloaded on 13/05/2010 at 18:21

Please note that terms and conditions apply.

J. Phys.: Condens. Matter **8** (1996) L421–L426. Printed in the UK

LETTER TO THE EDITOR

Looking for the maximum low-temperature conductivity in selectively doped $Al_xGa_{1-x}As$–GaAs–$Al_xGa_{1-x}As$ double heterojunctions

C D Simserides and G P Triberis

University of Athens, Department of Physics, Section of Solid State Physics, Panepistimiopolis, 157 84 Zografos, Athens, Greece

Received 28 May 1996

Abstract. We use self-consistent numerical calculations to study the sheet electron concentration and the mobility as functions of the doping concentration, the spacer thickness, the well width and the Al mole fraction of a selectively doped $Al_xGa_{1-x}As$/GaAs/$Al_xGa_{1-x}As$ double heterojunction, using no arbitrary, *a priori*, assumptions, at low temperatures.For the first time we take into account two kinds of donor (shallow and deep) that coexist in the Si-doped $Al_xGa_{1-x}As$. We study all the significant scattering mechanisms. The model, based exclusively upon the knowledge of the material and structural parameters involved, allows us to obtain the maximum conductivity for any specific structure. Our results are in a very good agreement with experiment.

From the early '80s the electron mobility (μ) of selectively doped $Al_xGa_{1-x}As$–GaAs heterostructures has been extensively studied both experimentally and theoretically. In the theoretical studies it is usually assumed that there exists a specific sheet electron concentration (n) or a specific number of subbands in the well or envelope functions of a certain form or a quantum well of a specific shape, etc. These simplifying hypotheses have been commonly used in one way or another [1–19]. The mobility is expressed as a 'function' of n but this procedure is limited by the arbitrary way of changing n. Characteristically, even when n is kept constant, it has been shown by experimentally [20] that the change in the shape of the envelope function (by varying the gate voltage) will change μ by up to 56%. Thus, the use of the above simplifying hypotheses can lead to erroneous conclusions. This imposes the necessity for the use of a model for the calculation of the electronic states that does not depend on such hypotheses.

A model that depends only on the material and structural parameters was first introduced by Hurkx and van Haeringen [21], for the case of selectively doped single heterojunctions. This model was generalized by Simserides and Triberis [22] for selectively doped double heterojunctions. There, we demonstrated self-consistently and numerically that the variation of the well width results in a dramatic change of the form of the envelope functions [22], due to the transition from a perfect 'square well' to a system of two independent heterojunctions. We also studied the effect of the variation of the doping concentrations and the width of the spacers on the electronic states. A similar model [23] was used in the study of the effect of delta doping in double heterojunctions. These models are presented at $T = 0$ K and they use the depletion approximation. Similar models have been successfully used to study the electronic structure of $Al_xGa_{1-x}As$–GaAs–$Al_xGa_{1-x}As$ quantum wells subjected to magnetic fields [24–26]. We have also shown [27] that, in order to study properly the

0953-8984/96/300421+06$19.50 © 1996 IOP Publishing Ltd

effect of temperature on the electronic states, one has to abandon the depletion approximation and to take into account the two kinds of donor (shallow and deep) which coexist in the Si-doped $Al_xGa_{1-x}As$ and are ionized by different mechanisms. Because of the fact that our models depend exclusively upon the knowledge of the parameters of the materials which constitute the heterostructure, we are able to study μ and n as functions of the doping concentrations, the spacer thicknesses, the well width and the Al mole fraction, using no arbitrary, *a priori*, assumptions. Even though many mobility calculations have been presented for the $Al_xGa_{1-x}As$–GaAs heterostructures, such an approach seems to be lacking in the literature.

It is the purpose of the present letter to show that even for material parameter values for which there is only one subband in the well there exist different n dependences of μ. For this case we are looking for the maximum conductivity, at low temperatures. The value of the maximum conductivity is of great importance when using these structures as FETs. All the significant scattering mechanisms are taken into account. Our results are compared with experimental data [17].

We use the normalized envelope functions given by

$$\varphi_i(\boldsymbol{r}) = (1/\sqrt{S})\zeta_i(z)\,\exp\big[\mathrm{i}\big(k_x x + k_y y\big)\big] \tag{1}$$

where S is the area of the interface (xy-plane). $\zeta_1(z)$ is the z-axis envelope function. $E = E_1 + \hbar^2k^2/2m^*$, where E_1 is the bottom of the subband, and $\boldsymbol{k} = (k_x,\, k_y)$ is the two-dimensional wavevector. The GaAs effective mass is $m^* = 0.067m_e$, where m_e is the electron mass. $\hbar$ is the reduced Planck constant.

The electron mobility reads

$$\mu = \big(e/m^*\big)\langle\phi(E)\rangle \tag{2}$$

where $(-e)$ is the electron charge.

$$\langle\phi(E)\rangle = \int \phi(E)E\frac{\partial f_0(E)}{\partial E}\,\mathrm{d}E \bigg/ \int E\frac{\partial f_0(E)}{\partial E}\,\mathrm{d}E. \tag{3}$$

The conductivity is given by

$$\sigma = \mu e n. \tag{4}$$

In the low-temperature range, we consider only the elastic scattering mechanisms.

For interface roughness (IR)

$$\frac{1}{\phi(E)} = \frac{m^*\Delta^2\Lambda^2}{2\hbar^3}\left\{U_0\Big[\zeta_1(z)^2\Big]_{z=z_B} + \frac{\hbar^2}{2m^*}\left[\left(\frac{\mathrm{d}\zeta_1(z)}{\mathrm{d}z}\right)^2\right]_{z=z_B}\left(1 - \frac{m^*_{AlGaAs}}{m^*}\right)\right\}^2 \times\left[\int_0^{2\pi}\mathrm{d}\theta\,(1-\cos\theta)\left[\left(\frac{1}{\epsilon(q)}\right)^2\exp\left(-\frac{q^2\Lambda^2}{4}\right)\right]_{q=2k\sin(\theta/2)}\right]. \tag{5}$$

Here, Δ is the roughness height and Λ is the roughness lateral size. m^*_{GaAlAs} is the $Al_xGa_{1-x}As$ effective mass. The values we use for the $Al_xGa_{1-x}As$ effective masses are taken from [28] by interpolation. U_0 is the conduction band offset. z_B denotes the position of the interface. Following Price and Stern [29] we take into account the fact that in the case of $Al_xGa_{1-x}As$–GaAs heterostructures, and especially when the Al mole fraction, x, is small, one has to assume a finite barrier at the interface. $\epsilon(q)$ is the RPA dielectric function.

For scattering due to deformation potential (DF)

$$\frac{1}{\phi(E)} = \frac{D^2k_BTm^*}{2\pi\hbar^3C_L}\int_{-\infty}^{+\infty}\mathrm{d}z\,\big(\zeta_1(z)\big)^4\int_0^{2\pi}\mathrm{d}\theta\,(1-\cos\theta)\left[\frac{1}{\epsilon(q)^2}\right]_{q=2k\sin(\theta/2)} \tag{6}$$

where $D = 7$ eV is the deformation potential constant and $C_L = 1.397 \times 10^{11}$ N m^{-2} is the longitudinal elastic constant. k_B is the Boltzmann constant.

For piezoelectric scattering (PZ)

$$\frac{1}{\phi(E)} = \frac{m^*}{(2\pi)^2\hbar^3} \frac{e^2 k_B T P^2}{2\varepsilon\varepsilon_0} \int_0^{2\pi} \mathrm{d}\theta \, (1-\cos\theta) \left[\frac{1}{\epsilon(q)^2}\mu(q)\right]_{q=2k\sin(\theta/2)} \tag{7}$$

where

$$\mu(q) = \int \mathrm{d}q_z \frac{1}{q^2+q_z^2} \left|I_{11}(q_z)\right|^2 \qquad I_{11}(q_z) = \int \zeta_1(z)\zeta_1(z) \, \exp(-\mathrm{i}q_z z) \, \mathrm{d}q_z.$$

$P = 0.052$ is the piezoelectric constant, $\varepsilon = 13.18$ is the GaAs dielectric constant and ε_0 is the vacuum dielectric constant.

For ionized impurities (II) we have

$$\frac{1}{\phi(E)} = \frac{m^*}{2\pi\hbar^3} \int \mathrm{d}z_i \, N_d^+(z_i) \int_0^{2\pi} \mathrm{d}\theta \, (1-\cos\theta) f(q, z_i)\big|_{q=2k\sin(\theta/2)} \tag{8}$$

where $N_d^+(z_i)$ is the ionized donor concentration at the position z_i.

$$f(q, z_i) = \left(\frac{e^2}{2\varepsilon_0\varepsilon}\right)^2 \left(\frac{1}{q\epsilon(q)}\right)^2 \left|F_I(q, z_i)\right|^2 \qquad F_I(q, z_i) = \int \mathrm{d}z \, \zeta_1(z)^2 \, \mathrm{e}^{-q|z-z_i|}.$$

For alloy scattering (AL)

$$\frac{1}{\phi(E)} = \left[\Omega_0 x(1-x)[\delta V]^2 \frac{m^*}{\hbar^3}\right] \int_{\mathcal{L}} \left(\zeta_1(z)\right)^4 \mathrm{d}z. \tag{9}$$

Here $4\Omega_0 = \alpha^3$, where α is the lattice constant. $\delta V = 1$ eV is the alloy potential. $\mathcal{L}$ denotes that the integral is performed only in the alloy.

Finally, we use Matthiessen's rule to estimate approximately the total mobility.

Figure 1 summarizes our results. In figure 1(a)–(d) the structures consist of an Si-doped $Al_{0.27}Ga_{0.73}As$ layer of doping concentration N_d, an undoped $Al_{0.27}Ga_{0.73}As$ spacer of width D_s, an undoped GaAs well of width $2L$, an undoped $Al_{0.27}Ga_{0.73}As$ spacer of width D_s and an Si-doped $Al_{0.27}Ga_{0.73}As$ layer of doping concentration N_d. We use $\Delta = 0.283$ nm, $\Lambda = 50$ nm for the normal interface (IR(n)) and $\Delta = 0.283$ nm, $\Lambda = 10$ nm for the inverted interface (IR(i)).

In figure 1(a) we present n, the mobilities due to the various scattering mechanisms and the total mobility, varying the width of the spacers. Here $N_d = 2 \times 10^{18}$ cm^{-3}, $2L = 8$ nm and $T = 25$ K.

In figure 1(b) we present n, the mobilities due to the various scattering mechanisms and the total mobility, varying the doping concentrations of the Si-doped layers. Here $D_s = 10$ nm, $2L = 8$ nm and $T = 25$ K.

In figure 1(c) we present n, the mobilities due to the various scattering mechanisms and the total mobility, varying the well width. Here $D_s = 10$ nm, $N_d = 1 \times 10^{18}$ cm^{-3} and $T = 25$K.

Figure 1(d) shows the different forms of the n dependence of μ. We observe that the variations of D_s (dashed line) leads to almost the same dependence as the variation of N_d (full line). This results from the fact that the shape of the envelope function depends only slightly on N_d or D_s for a given well width, $2L$ [22]. In contrast, when we vary $2L$ we observe a drastic change in the shape of the envelope function [22]. Thus, even for material parameter values for which we have only one subband in the well, we have a totally different form of n dependence of μ. We notice that variation of $2L$ in the range of 4–10 nm leads to almost ten times larger mobility ((0.039–0.30)$\times 10^6$ cm^2 V^{-1} s^{-1}). We also notice that the

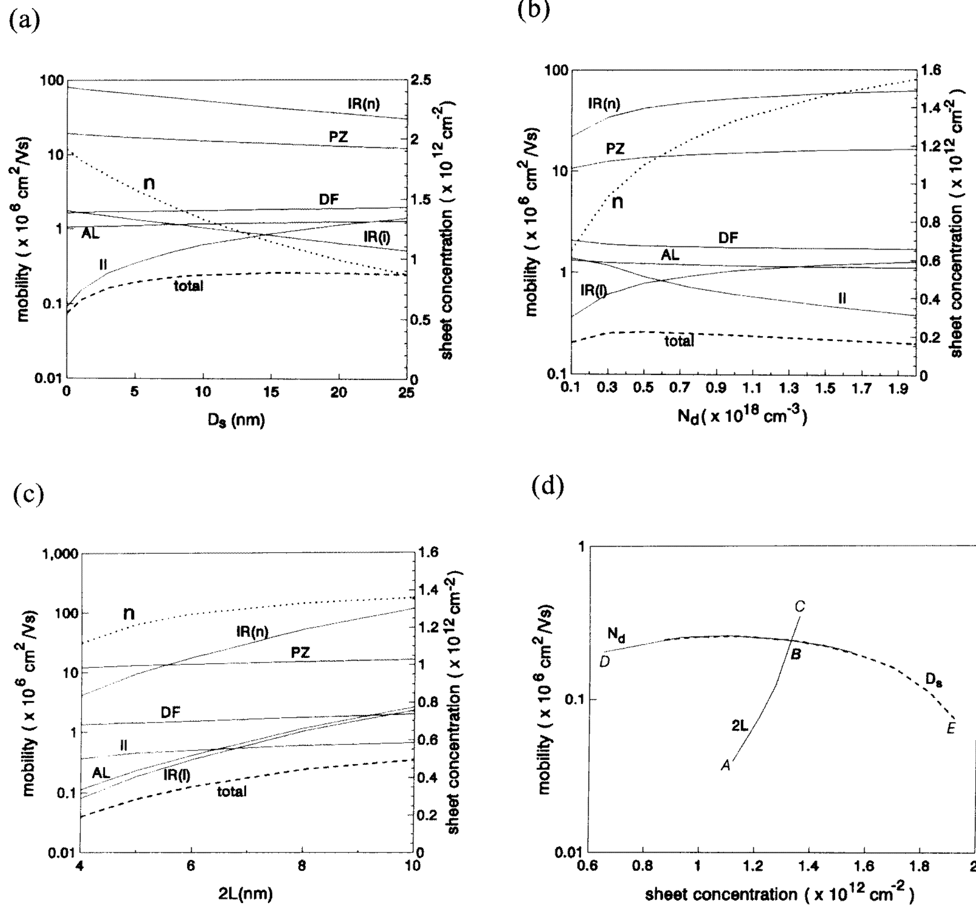

Figure 1. (a) The sheet electron concentration (n), the mobilities due to the various scattering mechanisms and the total mobility, varying the width of the spacers. $N_d = 1 \times 10^{18}$ cm^{-3}, $2L = 8$ nm, $T = 25$ K, $x = 0.27$. (b) n, the mobilities due to the various scattering mechanisms and the total mobility, varying the doping concentrations of the Si-doped layers. $D_s = 10$ nm, $2L = 8$ nm, $T = 25$ K, $x = 0.27$. (c) n, the mobilities due to the various scattering mechanisms and the total mobility, varying the well width. $D_s = 10$ nm, $N_d = 1 \times 10^{18}$ cm^{-3}, $T = 25$ K, $x = 0.27$. (d) Summarizing (a)–(c): the different forms of the n dependence of μ. The variation of D_s (dashed line) leads to almost the same dependence as the variation of N_d (full line). The variation of $2L$ results in a totally different behaviour. (e) $\langle\Phi(E)\rangle^{-1}$ as a function of $2L$ according to Bockelmann's experiment for $x = 0.35$ (dots) and our theoretical results (full line).

variation of $2L$ results in a significant variation of the conductivity. In this specific example σ is increased almost 11-fold, increasing $2L$. Specifically $\sigma_A = 0.071 \times 10^{-1}$C V^{-1} s^{-1}, $\sigma_B = 0.517 \times 10^{-1}$ C V^{-1} s^{-1} and $\sigma_c = 0.762 \times 10^{-1}$ C V^{-1} s^{-1}. In contrast, variation of N_d or D_s results in a much weaker effect. In this specific example by variation of N_d or D_s the conductivity can be increased approximately 2.5-fold. Specifically $\sigma_D = 0.208 \times 10^{-1}$ C V^{-1} s^{-1}, $\sigma_B = 0.517 \times 10^{-1}$ C V^{-1} s^{-1} and $\sigma_E = 0.230 \times 10^{-1}$ C V^{-1} s^{-1}. In this way we are able to obtain the maximum conductivity for the specific structure.

In figure 1(e) we compare our results (full line) with the experiment of Bockelmann *et al* [17] (points). In this experiment the structure is a superlattice of GaAs wells

(e)

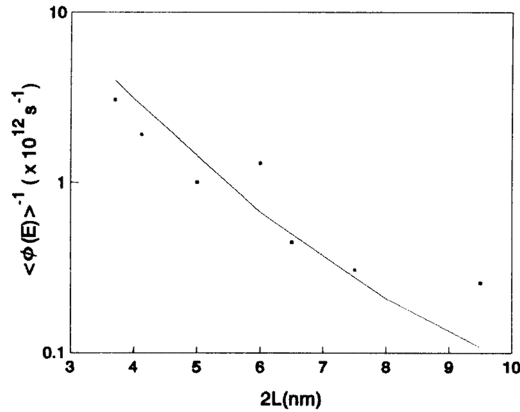

Figure 1. Continued.

separated by $Al_{0.35}Ga_{0.65}As$ barriers of typically 50 nm thickness. The central parts (10 nm) of the barriers are Si doped. The experimental conditions (variation of the doping concentrations and illumination) are such that the sheet electron concentration is kept constant at 0.65×10^{12} cm^{-2}/quantum well. Note that here the shape of the envelope function remains unchanged because it depends basically on the well width, $2L$ [22], while $N_d^+(z_i)$ varies. We use $\Delta = 0.283$ nm, $\Lambda = 50$ nm for the normal interface and $\Delta = 0.566$ nm, $\Lambda = 10$ nm for the inverted interface.

Using the arguments presented above the material and structural parameters which give maximum conductivity can be determined before the preparation of the actual heterostructure. This enables us to choose the most suitable combination of N_d, D_s and $2L$ to obtain the desired sheet concentration, mobility and conductivity.

References

[1] Ando T 1982 *J. Phys. Soc. Japan* **51** 3900
[2] Hirakawa K and Sakaki H 1986 *Phys. Rev.* B **33** 8291
[3] Walukiewicz W, Ruda H E, Lagowski J and Gatos H C 1984 *Phys. Rev.* B **30** 4571
[4] Price P J 1982 *Surf. Sci.* **113** 199
[5] Hess K 1979 *Appl. Phys. Lett.* **35** 484
[6] Fishman G and Calecki D 1984 *Phys. Rev.* B **29** 5778
[7] Fishman G 1983 *Phys. Rev.* B **27** 7611
[8] Price P J 1981 *J. Vac. Sci. Technol.* **19** 599
[9] Gold A 1987 *Phys. Rev.* B **35** 723
[10] Efros A L, Pikus F G and Samsonidze G G 1990 *Phys. Rev.* B **41** 8295
[11] Yokoyama K and Hess K 1986 *Phys. Rev.* B **33** 5595
[12] Okuyama Y and Tokuda N 1989 *Phys. Rev.* B **40** 9744
[13] Lin B J F, Tsui D C, Paalanen M A and Gossard A C 1984 *Appl. Phys. Lett.* **45** 695
[14] Price P J 1981 *Ann. Phys.* **133** 217
[15] Price P J 1984 *Surf. Sci.* **143** 145
[16] Guillemot C, Baudet M, Gauneau M, Regreny A and Portal J C 1987 *Phys. Rev.* B **35** 2799
[17] Bockelmann U, Abstreiter G, Weimann G and Schlapp W 1990 *Phys. Rev.* B **41** 7864
[18] Gold A 1989 *Solid State Commun.* **70** 371
[19] Gold A 1989 *Z. Phys.* B **74** 53

[20] Hirakawa K, Sakaki H and Yoshino J 1985 *Phys. Rev. Lett.* **54** 1279
[21] Hurkx G A M and van Haeringen W 1985 *J. Phys. C: Solid State Phys.* **18** 5617
[22] Simserides C D and Triberis G P 1993 *J. Phys.: Condens. Matter* **5** 6437
[23] Xu W and Mahanty J 1994 *J. Phys.: Condens. Matter* **6** 4745
[24] Xu W 1994 *Phys. Rev.* B **50** 14 601
[25] Xu W 1995 *Phys. Rev.* B **51** 9770
[26] Smrcka L and Jungwirth T 1995 *J. Phys.: Condens. Matter* **7** 3721
[27] Simserides C D and Triberis G P 1995 *J. Phys.: Condens. Matter* **7** 6317
[28] Watanabe M O and Maeda H 1984 *Japan. J. Appl. Phys.* **23** L734
[29] Price P J and Stern F 1983 *Surf. Sci.* **132** 577